Received: 6 December 2022 | Revised: 25 May 2023 | Accepted: 12 July 2023

DOI: 10.1002/gdj3.213

DATA ARTICLE

Geoscience Data Journal RMetS WILEY

# A database of detrital zircon U–Pb ages and Hf isotopic compositions from the Tarim, West Kunlun, Pamir, Tajik and Tianshuihai terranes

**Shijie Zhang**[1] | **Xiumian Hu**[2] | **Jinrong Zhang**[1] | **Qing Li**[1] | **Yiwei Xu**[3] | **Yuyang Yu**[1] | **Liqin Han**[1]

[1]College of Tourism, Henan Normal University, Xinxiang, China

[2]School of Earth Sciences and Engineering, Nanjing University, Nanjing, China

[3]Nanjing Institute of Geology and Palaeontology, Chinese Academy of Sciences, Nanjing, China

**Correspondence**
Shijie Zhang, College of Tourism, Henan Normal University, Xinxiang, China.
Email: zhangshijiex@foxmail.com

**Funding information**
National Key Research and Development Program, Grant/Award Number: 2022YFF0711704; National Natural Science Foundation of China, Grant/Award Number: 42050102 and 42102120

**Abstract**

With the development of detrital zircon U–Pb ages and Hf isotope analysis as conventional sedimentological research methods, a large number of studies have been conducted in the Tarim, West Kunlun, Tajik, Pamir and Tianshuihai regions and abundant data have been accumulated. Summarizing these data to characterize sedimentary units and source regions is more important than local studies of specific geological epochs; therefore, we compiled a database of detrital zircon U–Pb ages and Hf isotope analyses from the Tarim, West Kunlun, Pamir, Tajik and Tianshuihai terranes. The database contains data from 90 papers, including 35,281 individual U–Pb ages and 4,181 Hf isotope analyses. The database records the literature source, petrologic sample information, regional geological information, geographic coordinates and analytical parameters for each data point in as much detail as possible to allow readers to review, process, analyse and use the data. The database relies on the Deep-time Digital Earth (DDE) platform and uses an open database update system to enable sharing and collaborative building. We encourage other researchers to contribute relevant published data to facilitate wider use.

**KEYWORDS**

detrital zircon, Hf isotopes, Tajikistan, U–Pb ages, Xinjiang

## 1 | INTRODUCTION

Owing to its extreme resistance to weathering, zircon is found in many rocks, especially sedimentary rocks. It also has a high isotopic closure temperature and low fission track and (U–Th)/He closure temperatures, preserving a wealth of geological information about the timing of mineral formation, exhumation and cooling (George, 2014; Reiners & Brandon, 2006; Wu et al., 2007). Therefore, U–Pb dating, isotope analysis and low-temperature thermochronology of zircon are rapidly developing into essential tools in Earth science.

**Dataset** URL of dataset: https://repository.deep-time.org/detail/1598512745766391810

DOI of dataset: 10.12297/dpr.dde.202212.1

In the Tarim, West Kunlun, Pamir, Tajik and Tianshuihai terranes, the U–Pb ages and Hf isotopic compositions of detrital zircons in sedimentary and metasedimentary rocks have been used to reconstruct provenance (He et al., 2014; Wang et al., 2020), identify crustal components and understand the evolution of the crust (Long et al., 2019; Xu et al., 2013) and characterize sedimentary units and their source regions (Han et al., 2016; Zhang, Hu, & Garzanti, 2019). Detrital zircons provide a valuable opportunity to understand the formation and evolution of the Tarim Craton (Ge et al., 2014), reconstruct the tectonic evolution of the Tibet–Pamir Plateau and the Central Asian Orogenic Belt and correlate units between the Pamir and Tibet terranes.

To answer these major scientific questions, we must clarify the overall characteristics and evolutionary trends of geological units using 'big data'. Although local studies of specific geological periods have produced a large amount of data, a 'big data' approach has not been attempted to date. Therefore, we compiled a database of detrital zircon U–Pb ages and Hf isotopic compositions for Tarim, West Kunlun, Pamir, Tajik and Tianshuihai. The database contains 411 detrital zircon U–Pb age samples including 35,281 individual grains and 86 Hf isotopic composition samples including 4,181 individual grains. The original citation, sample petrology, geological setting, coordinates and analytical parameters for each analysis are recorded in detail in the database. We then performed simple calculations and error tests on the analytical data. Finally, we released the whole database publicly on the Deep-time Digital Earth (DDE) platform for readers to browse, download, share and use.

We expect that the data set will be useful for multiple purposes, including: (1) investigating the formation and evolution of the Tarim Craton by comparing the U–Pb ages and Hf isotopic characteristics of detrital zircons in different areas to study the assembly and breakup of supercontinents; (2) investigating the paleogeographic affinities between the Pamir and Tibet tectonic units; (3) reconstructing the palaeohydrological evolution of the Tarim Basin using the U–Pb ages and Hf isotopic compositions of detrital zircon grains to characterize sedimentary units.

## 2 | DATA PROCESSING AND DESCRIPTION

### 2.1 | Data coverage

The samples in the database were collected from Tajikistan and the Xinjiang Uygur Autonomous Region, China. The Xinjiang samples only include those collected from south of the North Tarim Fault. The geological units covered in the database are the Tarim, Western Kunlun, Pamir, Tajik and Tianshuihai terranes (Figure 1), and we exclude the Dunhuang Terrane to the east and the Altyn Tagh arc–basin system to the southeast.

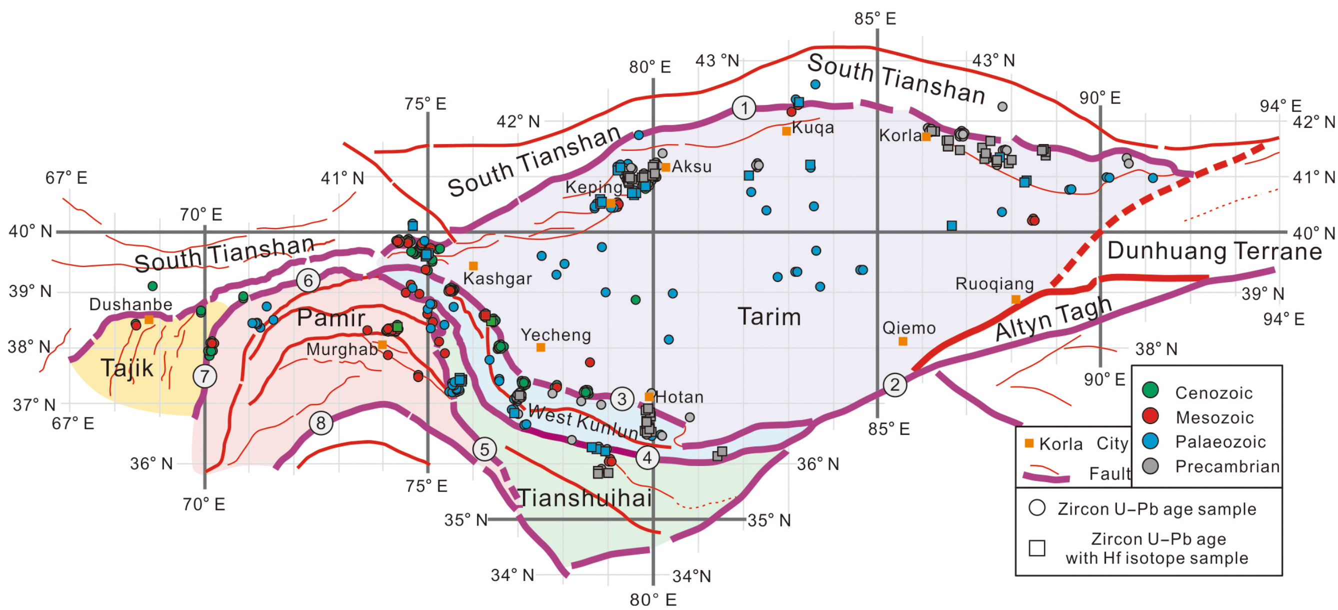


FIGURE 1 Distribution of detrital zircon U–Pb ages and Hf isotopic samples in the Tarim, West Kunlun, Pamir, Tajik and Tianshuihai terranes. Main faults separating the terranes: 1: North Tarim Fault, 2: Altyn Tagh Fault, 3: Tekilik Fault, 4: Karakax Fault, 5: Karakoram Fault, 6: Main Pamir Thrust Fault, 7: Darvaz Fault, 8: Tirich–Kilik Fault.

## 2.2 | Literature information

The database contains 90 published papers and master's and doctoral theses. 52 papers in English were collected from the Web of Science, and 38 papers in Chinese were compiled from the China National Knowledge Infrastructure (CNKI). Data were extracted from the main text and appendixes of the papers. The database includes details of all published articles, lead author, journal, volume, pages and a web link, thus allowing readers to locate the original studies. All relevant information about the Chinese literature is translated, and papers are identified as in Chinese with an English abstract in the Comments column.

## 2.3 | Lithology

The rock types in the database are limited to sedimentary and metasedimentary rocks. Metasedimentary rocks are not included in the database if the ages of detrital zircons have been completely reset by metamorphism. The lithological information includes rock type, lithostratigraphic unit and depositional age. In a few cases, authors differ in their interpretations of the geological ages of samples obtained within the same lithostratigraphic unit (Sun et al., 2016; Sun & Liu, 2006; Zheng et al., 2015). Our approach was to accept the geological age given by the authors; therefore, some stratigraphic units have different geological ages within the database.

## 2.4 | Geologic units

Based on previous studies, the area covered by the database is divided into five major tectonic units: the Tarim, West Kunlun, Pamir, Tajik and Tianshuihai terranes (Cowgill, 2010). Furthermore, the Tarim is divided into 15 (Qi et al., 2020), the West Kunlun is divided into two (North and South Kunlun), and the Pamir is divided into three (North, Central and South Pamir) subordinate tectonic units (Chapman et al., 2018; Schwab et al., 2004; Zhang, Zou, et al., 2019). Where samples are located near the boundary of two tectonic zones, are jointly influenced by both or their tectonic affinity is unclear, the database combines the names of the two tectonic units. For example, the frontal thrust zone of the West Kunlun is also a part of the Southwest Depression in the Tarim Basin; therefore, we recorded 'Tarim Basin–West Kunlun' in the geologic–geographic unit column for samples from this zone.

## 2.5 | Geographic location

Information about geographic location in the database includes sample coordinates, names of sedimentary sections and the administrative divisions to which they belong. The original authors expressed the coordinates in multiple formats (e.g., degree, minute, second and decimal degree formats), and these are presented in sheet 1 of each table. For ease of use, the database converts all coordinates to decimal degrees in sheet 2.

The database does not assess the accuracy of the coordinates presented in the original papers (presented in black in the coordinates column). However, some authors did not provide specific coordinates, which required us to extract them from maps in the papers. We present the coordinates that have an accuracy of $<1'$ on the map in the original paper in blue in the coordinate column; those whose accuracy is $<1°$ are shown in green, and those with accuracy $>1°$ are shown in red.

The country and region (province) where each sample was collected were easily determined. However, the locality or town of the sample location is often difficult to accurately identify, even for local scholars. Therefore, the database does not always express the actual administrative district where the sample was collected in the locality column but presents a nearby well-known town. This enables the readers to quickly find the approximate sampling location by locating the town.

## 2.6 | Detrital zircon U–Pb ages

The data for detrital zircon in the U–Pb age table include isotopic ratios, U and Th contents (ppm), Th/U ratios, U–Pb ages and discordance ratios. Although the authors use different ways of presenting the uncertainty in isotopic ratios, selecting the confidence interval range and calculating the best estimate and uncertainty in the age and discordance ratio, we chose to present the original data in sheet 1 of the detrital zircon U–Pb age table.

To address the shortcomings in the format of the data in sheet 1, we standardized the format of the uncertainty in isotopic ratios and confidence intervals in sheet 2. Assuming that the U–Pb age provided by the original authors is accurate, we recalculated the best age, discordance ratio and Th/U ratio using a single method, including recalculating the ages that were discarded by the authors owing to discordance. The best U–Pb age were chosen depending on whether the detrital zircon was older than 1,200 Ma: 207Pb/206Pb ages are used for zircons older than 1,200 Ma while the 206Pb/238U ages for younger zircons. Finally, the database presents the best age with <30% discordance as the recommended value in sheet 2 for ease of use and to allow direct comparisons.

### 2.7 | Detrital zircon Hf isotope analyses

The data in the table of detrital zircon Hf isotopic analyses include both raw analytical mass spectrometer data and the results of calculations based on them. Differences in the recommended value of the $^{176}$Lu decay constant used by different authors inevitably led to differences in the calculated results, affecting comparisons between different data (Wu et al., 2007). However, we still choose to present the results of the calculations carried out by the original authors in sheet 1.

To resolve the problem of using different decay constants, we recalculated the raw analytical data using a $^{176}$Lu decay constant ($\lambda$) of $1.867 \times 10^{-11}$ $y^{-1}$ (Söderlund et al., 2004). The Hf isotopic parameters commonly used in petrogenetic and geodynamic studies [e.g., the initial $^{176}Hf/^{177}Hf$ ratio, εHf(0) and εHf(t) values and Hf model age ($T_{DM1}$) and two-stage model age ($T_{DM2}$)] are presented in sheet 2. The specific formulae, as well as the important parameters involved in the calculations, are described in detail in Wu et al. (2007).

## 3 | DATABASE DESCRIPTION

### 3.1 | Data volumes

The database consists of a table of detrital zircon U–Pb ages and a table of detrital zircon Hf isotopic compositions. Each table is composed of three sheets. The detrital zircon U–Pb age table contains 90 papers (from 2007 to 2022), including 411 samples and 35,281 individual ages (Table 1). The original raw data are presented in sheet 1. After standardizing the format and recalculating the best age and discordance, we obtained 34,506 zircon U–Pb ages with discordance <30% (Table 2). These data are presented in sheet 2 in a uniform format that can be directly used, analysed, and compared. Reliable detrital zircon age data were visualized using kernel density estimation (KDE) plots (Figure 2) drawn using IsoplotR software (Vermeesch, 2018). The detrital zircon Hf isotopic composition table contains 22 papers, including 86 samples and 4,181 individual analyses (Table 3). The raw analytical data and results provided by the authors are presented in sheet 1, and the recalculated results are presented in sheet 2 in a uniform format. Finally, all citations and sample information are summarized in sheet 3 of each table for quick reference.

**TABLE 1** Data volumes of the database of U–Pb ages of detrital zircons from the Tarim, West Kunlun, Pamir, Tajik and Tianshuihai terranes

| | | | | | |
|---|---|---|---|---|---|
| **Papers** | **90** | | | | |
| **Samples** | **411** | | | | |
| **Grains** | **35,281** | | | | |
| **Discordance >30%** | | **775** | **Discordance <30%** | | **34,506** |
| **Era/Eon** | **Samples** | **Grains** | **Period/Era** | **Samples** | **Grains** |
| Cenozoic | 110 | 11,205 | Quaternary | 1 | 100 |
| | | | Neogene | 70 | 6,403 |
| | | | Paleogene | 39 | 4,702 |
| Mesozoic | 50 | 6,368 | Cretaceous | 26 | 3,445 |
| | | | Jurassic | 7 | 391 |
| | | | Triassic | 17 | 2,532 |
| Palaeozoic | 115 | 8,872 | Permian | 21 | 1,682 |
| | | | Carboniferous | 8 | 657 |
| | | | Devonian | 26 | 1,900 |
| | | | Silurian | 22 | 1,740 |
| | | | Ordovician | 11 | 969 |
| | | | Cambrian | 17 | 752 |
| | | | Not subdivided | 10 | 1,172 |
| Precambrian | 136 | 8,061 | Neoproterozoic | 110 | 6,672 |
| | | | Mesoproterozoic | 8 | 484 |
| | | | Paleoproterozoic | 10 | 536 |
| | | | Not subdivided | 8 | 369 |

**TABLE 2** Summary of compiled standardized data from U–Pb ages and Hf isotope analyses of detrital zircon grains from the Tarim, West Kunlun, Pamir, Tajik and Tianshuihai terranes

| Terrane unit | Subdivide | Detrital zircon grains | Hf isotope grains of detrital zircon |
|---|---|---|---|
| Tarim Craton | Cenozoic | 8,421 | 90 |
| | Mesozoic | 1,585 | 76 |
| | Palaeozoic | 6,069 | 1,207 |
| | Precambrain | 5,076 | 1,514 |
| West Kunlun terrane | | 4,248 | 658 |
| Tianshuihai terrane | | 1,363 | 549 |
| Tajik Basin | | 2,521 | |
| Pamir terranes | North Pamir | 849 | |
| | Central Pamir | 1,559 | 36 |
| | Central Pamir, detratal zircon derive from South Pamir | 1,500 | |
| | South Pamir | 690 | |
| | Unclassified | 289 | |
| South Tianshan | | 336 | 51 |

## 3.2 | U–Pb ages of detrital zircon and their spatial and temporal distributions

### 3.2.1 | Tarim Craton

Precambrian samples are concentrated in the Kuruktag Uplift in the northeast, the Keping Uplift in the northwest and the West Kunlun in the southwest of the Tarim Basin (Figure 1). This is consistent with the exposure of Precambrian metasedimentary rocks in the Kuruktag, Altyn Tagh (not included in the database), Tekilik and Aksu areas on the periphery of the Tarim Basin (Long et al., 2019; Wang et al., 2020; Xu et al., 2013). They show a distinct peak at 900–700 Ma, two secondary peaks at 2,100–1,760 Ma, and two smaller peaks at ~2,500 and ~640 Ma (Figure 2). Previous studies have proposed that they originated during the formation of the Tarim crust (Ge et al., 2014) and the assembly and breakup of the Columbia, Rodinia and Gondwana supercontinents (He et al., 2014; Wang et al., 2020).

Palaeozoic samples are found across the interior of the Tarim Basin (Figure 1). The ages of detrital zircons from these samples have two prominent peaks at 500–400 and 300–250 Ma and a smaller peak at ~960 Ma, in addition to the peaks seen in the Precambrian samples (Figure 2). The zircons in the two prominent age peaks are generally thought to have formed during magmatism associated with the formation, evolution and destruction of the Palaeo-Asian Ocean and the Proto- and Palaeo-Tethys oceans (Chapman et al., 2018; Han et al., 2016; Schwab et al., 2004; Zhang, Zou, et al., 2019).

Mesozoic samples are concentrated in the western Tarim Basin (Figure 1). Their detrital zircon ages, in addition to inheriting the characteristics of the Palaeozoic samples, are characterized by additional ages at 250–200 Ma (Figure 2). Owing to the closure of the South Tianshan Ocean, no magmatism occurred in the Tianshan orogenic belt after the Triassic (Han et al., 2016). However, Triassic magmatic rocks are commonly exposed in the North Pamir and Tianshuihai terranes and the Altyn Tagh Mountains (Zhang et al., 2021). This suggests that the source of these Triassic grains was the orogenic belt to the south of the basin.

Cenozoic samples are concentrated in the foreland thrust zone of the Western Kunlun and Pamir (Figure 1). This may be due to the fact that Cenozoic strata are well exposed in the foreland zone, whereas they are rare in the interior of the basin. Detrital zircons from Cenozoic samples have a small peak at 60–40 Ma (Figure 2). Regional studies have shown that Cenozoic magmatic rocks are exposed in the Central Pamir–Tianshuihai terrane (Chapman et al., 2018; Zhang et al., 2021; Zhang, Hu, & Garzanti, 2019). The occurrence of those detrital zircon ages reflects the tectonic evolution of the source area (Chapman et al., 2018; Schwab et al., 2004; Zhang, Hu, & Garzanti, 2019).

### 3.2.2 | West Kunlun terrane

The West Kunlun samples are mainly from Precambrian and Palaeozoic strata, with a small number from Mesozoic strata (Figure 1). The ages of the detrital zircon grains are very similar to those from the Palaeozoic–Mesozoic Tarim Basin samples. They all show three prominent peaks, at 900–700, 500–400 and 300–200 Ma (Figure 2). This is because the West Kunlun terrane is composed mainly of Tarim Craton basement and Precambrian and Palaeozoic–Mesozoic metasedimentary rocks (Long et al., 2019; Zhang, Zou, et al., 2019). The metasedimentary rocks were formed during the magmatism associated with the formation, evolution and destruction of the Proto- and Paleo-Tethys oceans (Schwab et al., 2004; Zhang, Hu, & Garzanti, 2019).

### 3.2.3 | Tianshuihai terrane

Precambrian and Palaeozoic samples from the Tianshuihai terrane were collected mainly from the area to the south

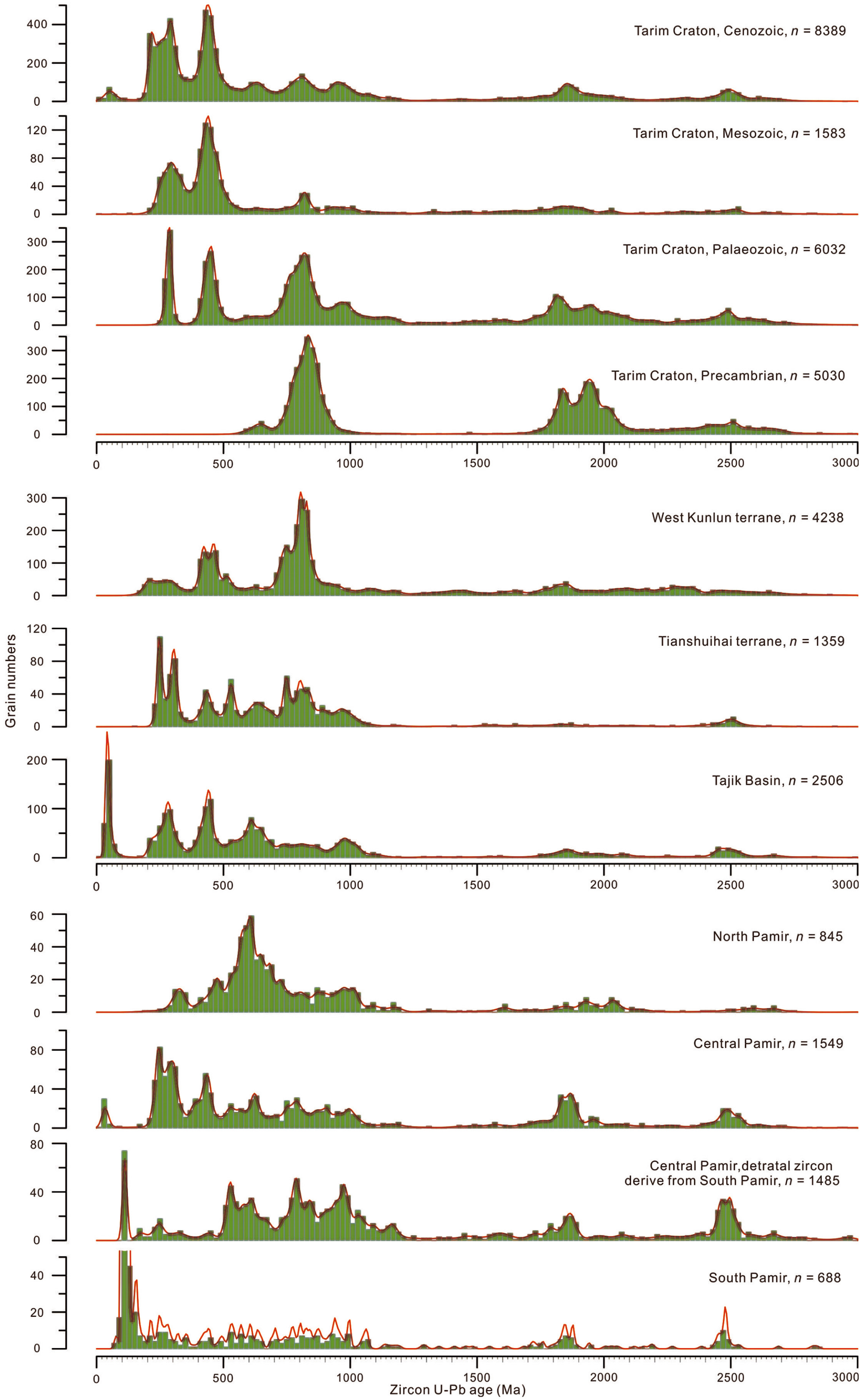


**FIGURE 2** The U–Pb age spectra histograms and kernel density estimation (KDE) plots of detrital zircon U–Pb ages from sedimentary and metasedimentary rock in the Tarim, West Kunlun, Pamir, Tajik and Tianshuihai terranes.

TABLE 3 Data volumes of the database of Hf isotope analyses of detrital zircon from the Tarim, West Kunlun, Pamir, Tajik and Tianshuihai terranes

| Papers | 22 | | | | |
|---|---|---|---|---|---|
| **Samples** | **87** | | | | |
| **Grains** | **4,181** | | | | |
| **Era/Eon** | **Samples** | **Grains** | **Period/Era** | **Samples** | **Grains** |
| Cenozoic | 3 | 126 | Quaternary | | |
| | | | Neogene | | |
| | | | Paleogene | 3 | 126 |
| Mesozoic | 1 | 76 | Cretaceous | 1 | 76 |
| | | | Jurassic | | |
| | | | Triassic | | |
| Palaeozoic | 31 | 1,625 | Permian | 10 | 698 |
| | | | Carboniferous | 2 | 113 |
| | | | Devonian | 5 | 93 |
| | | | Silurian | 5 | 321 |
| | | | Ordovician | 4 | 343 |
| | | | Cambrian | 4 | 45 |
| | | | Not subdivided | 1 | 12 |
| Precambrian | 52 | 2,354 | Neoproterozoic | 40 | 1827 |
| | | | Mesoproterozoic | 2 | 50 |
| | | | Paleoproterozoic | 10 | 477 |

of the Karakax Fault and from the Taxkorgan valley (Figure 1). The ages of the detrital zircon grains are similar to those from Palaeozoic strata in the Songpan–Ganzi terrane, characterized by two prominent peaks at 500–400 and 300–200 Ma (Li et al., 2020). However, it also shares three peaks with the Qiangtang terrane, at ~970, ~800 and 640–500 Ma (Li et al., 2020) (Figure 2), suggesting that the Tianshuihai terrane with affinity similar to the Songpan–Ganzi terrane to the east were also influenced by the Qiangtang terrane to the south.

### 3.2.4 | Tajik Basin

The samples from the Tajik Basin are mainly from Mesozoic–Cenozoic strata in northwestern Pamir (Figure 1) The ages of their detrital zircon grains are similar to those from Central Pamir strata, characterized by a distinct triple peak at 640–500, 500–400 and 300–200 Ma, although they have a more prominent peak at ~40 Ma (Figure 2). Regional studies have shown that Eocene magmatic rocks are exposed in Central Pamir (Chapman et al., 2018; Zhang et al., 2021; Zhang, Hu, & Garzanti, 2019). Therefore, we infer that the provenance of the Mesozoic–Cenozoic strata is Central Pamir, although it may also have been influenced by North Pamir.

### 3.2.5 | Pamir terranes

The North Pamir samples were collected mainly from the Kurgovat metamorphic complex (Figure 1). The primary peak at ~700 to 500 Ma and the broad peak at ~1,100 to 700 Ma are consistent with Pan-African age signatures (Figure 2), suggesting that the complex was once located on the northern margin of Western Gondwanaland (Li et al., 2020).

Central Pamir samples from different stratigraphic units exhibit two distinct detrital zircon characteristics (He et al., 2014). The zircon U–Pb ages of modern river sands and bedrock in Pamir show that Cenozoic magmatism is exposed mainly in Central Pamir, whereas mid-Cretaceous magmatism was distributed widely across South Pamir (Chapman et al., 2018; Zhang et al., 2021; Zhang, Hu, & Garzanti, 2019). Detrital zircon samples with two prominent peaks at 500–400 and 300–200 Ma and a small peak at ~20 Ma clearly reflect the characteristics of Central Pamir (Figure 2). Central Pamir samples with a prominent peak at 120–100 Ma and three peaks at ~970, ~800 and 640–500 Ma are consistent with detrital zircon from samples collected from South Pamir (Figure 2), suggesting that their provenance was South Pamir (He et al., 2019). Mid-Cretaceous magmatic rocks are exposed in the South Pamir and Qiangtang terranes (Chapman et al., 2018). A large broad peak at ~1,100 to 500 Ma with three peaks at ~970, ~800 and 640–500 Ma is a typical feature of the Qiangtang terrane (He et al., 2019). Therefore, we suggest that South Pamir has a paleogeographic affinity with the Qiangtang terrane.

### 3.3 | Hf isotopic compositions of detrital zircons and their spatial and temporal distributions

The detrital zircon Hf isotope samples in the database are predominantly Precambrian and Palaeozoic in age (Table. 3). They are mainly distributed in the Kuruktag Uplift in the northeast, the Keping Uplift in the northwest and the Western Kunlun in the southwest of the Tarim Basin (Figure 1). This supports our expectation that these data can be used to address scientific questions about the formation and evolution of the Tarim Craton and the assembly and breakup of supercontinents (He et al., 2014; Wang et al., 2020).

The detrital zircon Hf isotope samples in the database have seven major age populations at 2600–2200, 2050–1800, 950–700, 680–700, 500–400, 300–200 and 50–30 Ma (Figure 3). The zircon populations at 2600–2200, 2050–1800, 950–700 and 680–600 Ma yield some positive εHf(t) values, but they mostly record the reworking of ancient crustal material (εHf(t) values of less than −5) or juvenile input to the source areas (εHf(t) values of −5 to +5), consistent with the εHf(t) values of the Precambrian magmatic rocks in the Tarim basement (Han et al., 2015; He et al., 2014; Long et al., 2019; Wang et al., 2020). The detrital zircon populations at 500–400 and 300–200 Ma have a large range of εHf(t) values (−13 to +12), which largely overlap with those of the Palaeozoic magmatic rocks in the Tianshan and West Kunlun terranes (Han et al., 2015, 2016; Zhang, Hu, & Garzanti, 2019). The detrital zircon grains in the 50–30 Ma population have more positive εHf(t) values (−5 to +15), which are similar to those of igneous rocks from the Central Pamir Terrane (−5 to +5) and the Kohistan and Ladakh arcs (+2 to +15; Sun et al., 2016; Zhang, Hu, & Garzanti, 2019).

## 4 | POTENTIAL USES AND FUTURE EXPANSION OF THE DATA

### 4.1 | Potential data uses

Data in sheet 2 of the U–Pb age table and sheet 2 of the Hf isotopic composition table have been processed for consistency and can be compared directly. We recommend using lithostratigraphic units and tectonic terranes as the primary indicators of temporal and spatial correlation, respectively, although it is advisable to also refer to the geological age, coordinates and other geological and geographical data.

The choice of primary correlation indicators is based on two main considerations. (1) The classification and correlation of regional lithostratigraphic units are better established than their geological ages, although the geological ages of some lithostratigraphic units are debated (Sun et al., 2016; Sun & Liu, 2006; Zheng et al., 2015). (2) Terranes are defined by both their geographical location and geological affinities, implying that samples from the same terrane should be similar.

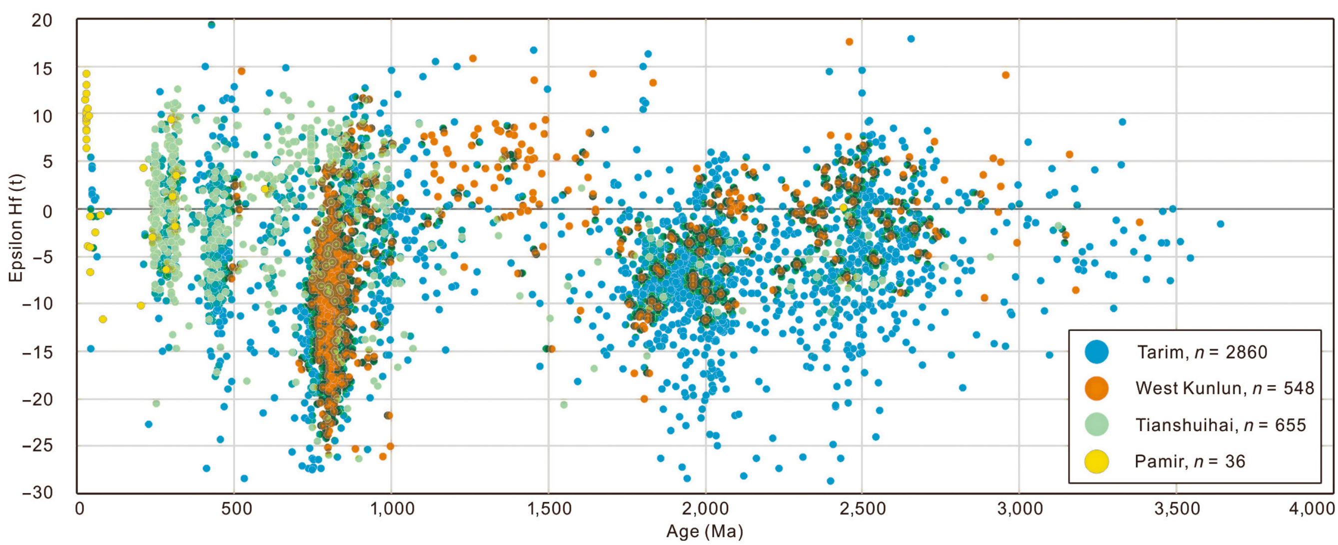


**FIGURE 3** Detrital zircon U–Pb age versus εHf(t) values for samples from the Tarim, West Kunlun, Pamir and Tianshuihai terranes.

### 4.2 | Future expansion

Wherever possible, the database includes all published detrital zircon data from the region, but we remain alert to papers that we may have overlooked. In addition, we note that many of the relevant papers do not provide the full analytical data, preventing us from expanding the database further.

Detrital zircon U–Pb ages and Hf isotope analyses are now conventional research methods in sedimentology, and more papers covering this topic will be published in the future. Therefore, the database relies on the DDE platform and uses an open database maintenance system based on the concept of sharing and building together. Although the authors will continue to maintain, update and expand the database in the future, we encourage other researchers to contribute their published data to facilitate their use by more people.

## AUTHOR CONTRIBUTIONS

**Shijie Zhang:** Data curation (equal); formal analysis (equal); investigation (equal); methodology (equal); validation (equal); writing – original draft (lead); writing – review and editing (equal). **Xiumian Hu:** Conceptualization (equal); funding acquisition (lead); project administration (lead); supervision (equal). **Jinrong Zhang:** Investigation (equal); resources (equal). **Qing Li:** Investigation (equal); resources (equal). **Yiwei Xu:** Formal analysis (equal); resources (equal); validation (equal); writing – original draft (supporting). **Yuyang Yu:** Resources (equal); software (equal); visualization (equal); writing – original draft (supporting). **Liqin Han:** Funding acquisition (supporting); resources (equal).

## ACKNOWLEDGEMENTS

We are grateful to Dr Hu Huang for his help in collecting and collating data from the Kuruktag Uplift. This work is supported by the National Natural Science Foundation of China (NSFC; 42050102 and 42102120), the Deep-time Digital Earth (DDE) Big Science Program and the National Key Research and Development Program (2022YFF0711704).

## CONFLICT OF INTEREST STATEMENT

The authors declare no conflict of interest.

## OPEN RESEARCH BADGES

This article has earned an Open Data badge for making publicly available the digital data necessary to reproduce the reported results. The data are available at https://repository.deep-time.org/detail/1598512745766391810. Learn more about the Open Practices badges from the Centre for Open Science: https://osf.io/tvyxz/wiki.

## ORCID

*Shijie Zhang* https://orcid.org/0000-0002-6973-493X
*Xiumian Hu* https://orcid.org/0000-0002-5401-8682

## REFERENCES

Chapman, J.B., Scoggin, S.H., Kapp, P., Carrapa, B., Ducea, M.N., Worthington, J. et al. (2018) Mesozoic to Cenozoic magmatic history of the Pamir. *Earth and Planetary Science Letters*, 482, 181–192.

Cowgill, E. (2010) Cenozoic right-slip faulting along the eastern margin of the Pamir salient, northwestern China. *GSA Bulletin*, 122, 145–161.

Ge, R., Zhu, W., Wilde, S.A. & He, J. (2014) Zircon U–Pb–Lu–Hf–O isotopic evidence for ≥3.5Ga crustal growth, reworking and differentiation in the northern Tarim craton. *Precambrian Research*, 249, 115–128.

George, G. (2014) Detrital zircon U-Pb geochronology applied to tectonics. *Annual Review of Earth and Planetary Sciences*, 42, 127–149.

Han, Y., Zhao, G., Sun, M., Eizenhöfer, P.R., Hou, W., Zhang, X. et al. (2015) Paleozoic accretionary orogenesis in the paleo-Asian Ocean: insights from detrital zircons from Silurian to carboniferous strata at the northwestern margin of the Tarim craton. *Tectonics*, 34, 334–351.

Han, Y., Zhao, G., Sun, M., Eizenhöfer, P.R., Hou, W., Zhang, X. et al. (2016) Late Paleozoic subduction and collision processes during the amalgamation of the central Asian Orogenic Belt along the south Tianshan suture zone. *Lithos*, 246-247, 1–12.

He, J., Kapp, P., Chapman, J.B., DeCelles, P.G. & Carrapa, B. (2019) Structural setting and detrital zircon U–Pb geochronology of Triassic–Cenozoic strata in the eastern central Pamir, Tajikistan. *Geological Society, London, Special Publications*, 483, 605–630.

He, J., Zhu, W., Ge, R., Zheng, B. & Wu, H. (2014) Detrital zircon U–Pb ages and Hf isotopes of Neoproterozoic strata in the Aksu area, northwestern Tarim craton: implications for supercontinent reconstruction and crustal evolution. *Precambrian Research*, 254, 194–209.

Li, Y., Robinson, A.C., Gadoev, M. & Oimuhammadzoda, I. (2020) Was the Pamir salient built along a late Paleozoic embayment on the southern Asian margin? *Earth and Planetary Science Letters*, 550, 116554.

Long, X., Xu, B., Yuan, C., Zhang, C. & Zhang, L. (2019) Precambrian crustal evolution of the southwestern Tarim craton, NW China: constraints from new detrital zircon ages and Hf isotopic data of the Neoproterozoic metasedimentary rocks. *Precambrian Research*, 334, 105473.

Qi, L., Li, Z. & Lv, H. (2020) *Atlas of structural sedimentary evolution and oil-gas exploration in Tarim superimposed basin*. Beijing: Science Press.

Reiners, P.W. & Brandon, M.T. (2006) Using thermochronology to understand orogenic erosion. *Annual Review of Earth and Planetary Sciences*, 34, 419–466.

Schwab, M., Ratschbacher, L., Siebel, W., McWilliams, M., Minaev, V., Lutkov, V. et al. (2004) Assembly of the Pamirs: age and origin of magmatic belts from the southern Tien Shan to the southern Pamirs and their relation to Tibet. *Tectonics*, 23(4), TC4002.

Söderlund, U., Patchett, P.J., Vervoort, J.D., Isachsen, C.E. & Letters, P.S. (2004) The $^{176}$Lu decay constant determined by Lu–Hf and U–Pb isotope systematics of Precambrian mafic intrusions. *Earth and Planetary Science Letters*, 219, 311–324.

Sun, J. & Liu, T. (2006) The age of the Taklimakan Desert. *Science*, 312, 1621.

Sun, J., Xiao, W., Windley, B.F., Ji, W., Fu, B., Wang, J. et al. (2016) Provenance change of sediment input in the northeastern foreland of Pamir related to collision of the Indian plate with the Kohistan-Ladakh arc at around 47 Ma. *Tectonics*, 35, 315–338.

Vermeesch, P. (2018) IsoplotR: a free and open toolbox for geochronology. *Geoscience Frontiers*, 9, 1479–1493.

Wang, P., Zhao, G., Liu, Q., Han, Y., Yao, J. & Li, J. (2020) Zircons from the Tarim basement provide insights into its positions in Columbia and Rodinia supercontinents. *Precambrian Research*, 341, 105621.

Wu, F., Li, X., Zheng, Y. & Gao, S. (2007) Lu-Hf isotopic systematics and their applications in petrology. *Acta Petrologica Sinica*, 23, 185–220.

Xu, Z., He, B., Zhang, C., Zhang, J., Wang, Z. & Cai, Z. (2013) Tectonic framework and crustal evolution of the Precambrian basement of the Tarim block in NW China: new geochronological evidence from deep drilling samples. *Precambrian Research*, 235, 150–162.

Zhang, C., Zou, H., Ye, X. & Chen, X. (2019) Tectonic evolution of the west Kunlun Orogenic Belt along the northern margin of the Tibetan plateau: implications for the assembly of the Tarim terrane to Gondwana. *Geoscience Frontiers*, 10, 973–988.

Zhang, S., Hu, X., Gao, Z., Zhao, Y., Ma, A. & Xu, Y. (2021) Palaeogene uplift and deformation in west Kunlun Mountains: timing, evidence and controversy. *Geological Review*, 67(4), 1057–1076.

Zhang, S., Hu, X. & Garzanti, E. (2019) Paleocene initial indentation and early growth of the Pamir as recorded in the western Tarim Basin. *Tectonophysics*, 772, 228207.

Zheng, H., Wei, X., Tada, R., Clift, P.D., Wang, B., Jourdan, F. et al. (2015) Late Oligocene–early Miocene birth of the Taklimakan Desert. *Proceedings of the National Academy of Sciences*, 112, 7662–7667.

**How to cite this article:** Zhang, S., Hu, X., Zhang, J., Li, Q., Xu, Y., Yu, Y. et al. (2024) A database of detrital zircon U–Pb ages and Hf isotopic compositions from the Tarim, West Kunlun, Pamir, Tajik and Tianshuihai terranes. *Geoscience Data Journal*, 11, 118–127. Available from: https://doi.org/10.1002/gdj3.213